Electronic Supporting Information (ESI)

A diboronic acid fluorescent sensor with fluorescence quenching selective recognition of D-ribose

Hao Wang,‡[a, b, c, d] Guiqian Fang,‡[a, b, c, d] Hongxiao Wang[a, b, c, d] Jindi Dou[a, b, c, d] Zhancun Bian,[a, b, c, d] Ying Li[a, b, c, d] Huining Chai[a, b, c, d] Zhongyu Wu*[a, b, c, d] and Qingqiang Yao*[a, b, c, d]

a. School of Medicine and Life Sciences，University of Jinan-Shandong Academy of Medical Sciences，Jinan 250200，Shandong，China

b. Institute of Materia Medica, Shandong Academy of Medical Sciences，Jinan 250062，Shandong，China

c. Key Laboratory for Biotech-Drugs Ministry of Health，Jinan 250062，Shandong，China

d. Key Laboratory for Rare & Uncommon Diseases of Shandong Province，Jinan 250062，Shandong，China

e. Department of Medicinal Chemistry, School of Pharmaceutical Sciences, Shandong University, Jinan, Shandong 250012, China

*Corresponding authors: E-Mail: wu_med@foxmail.com (Zhongyu Wu), yao_imm@163.com (Qingqiang Yao)

1. Synthesis of 2-(4-boronophenyl)quinoline-4-carboxylic acid (1)

This paper reports on the synthesis of PBAQA according to the preliminary work of our group,[1] as shown in Scheme 1. Starting from p-bromoacetophenone and eosin, PBAQA was synthesized by Pfitzinger Reaction, carboxyl esterification, palladium catalysis, hydrolysis, and so on. ^{1}H NMR (600 MHz, CD_3OD) δ (ppm) (Fig. S1): 8.83 (d, J = 8.5 Hz, 1H), 8.51 (s, 1H), 8.25 (d, J = 8.4 Hz, 1H), 8.12 (d, J = 7.6 Hz, 2H), 7.99 – 7.82 (m, 3H), 7.77 (t, J = 7.7 Hz, 1H). 13C NMR (151 MHz, CD_3OD) δ (ppm) (Fig. S2): 166.85, 156.33, 136.82, 134.17, 131.61, 128.48, 126.88, 125.99, 124.38, 120.82. ESI-MS (Fig. S3): m/z 294.0 [M+1]$^+$.

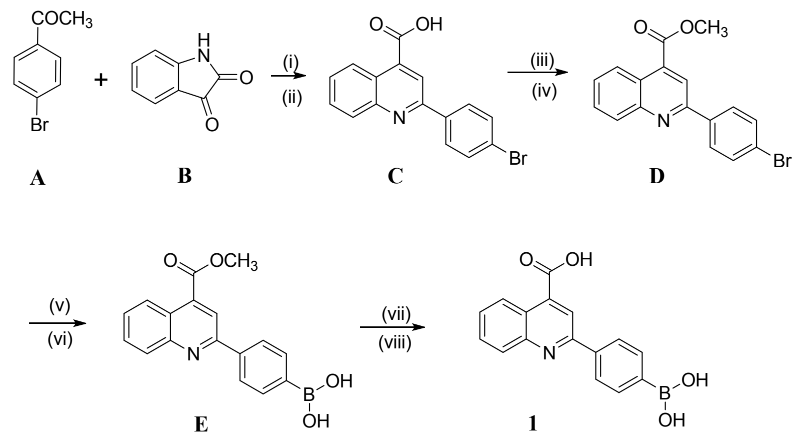

Scheme 1 Synthetic route of PBAQA.[1] (i) EtOH, KOH, rt, 8 h. (ii) HCl, rt, pH 3. (iii) $SOCl_2$, reflux, 4 h. (iv) Methanol, TEA, 0 °C, 1 h. (v) Pd-catalyst, KOAc, Bis(pinacolato)diboron, 75 °C, 8 h . (vi) $NaIO_4$, HCl, rt, 12 h. (vii) NaOH, 0 °C, 1 h. (viii) HCl, rt, pH 4.

2.Figure

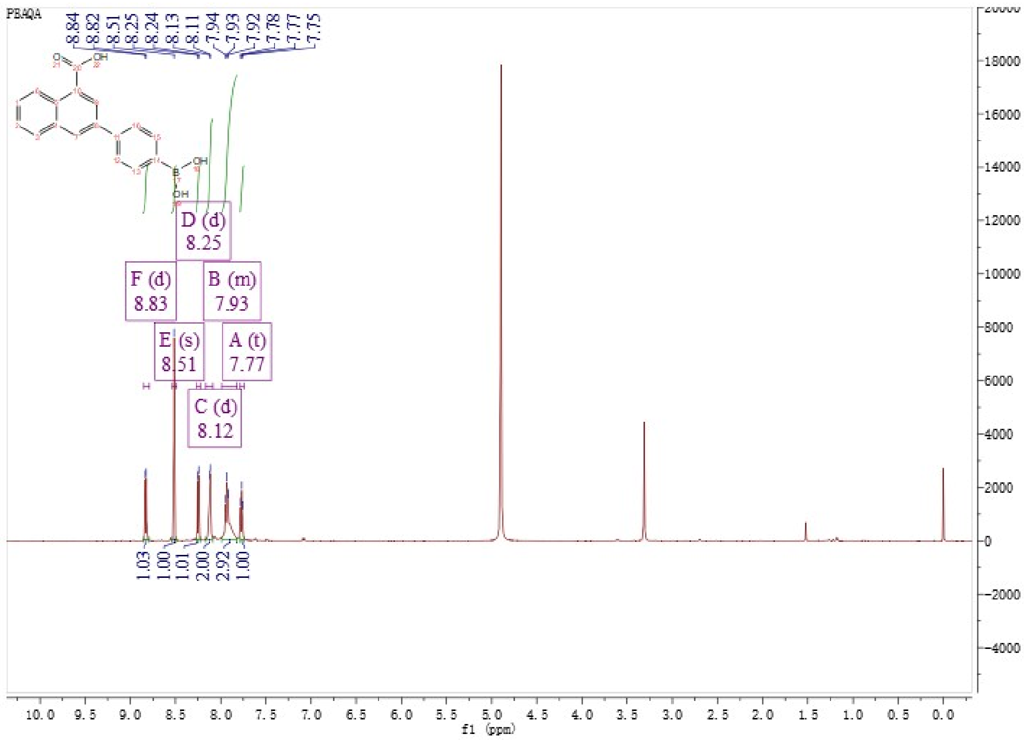

Fig. S1 ^{1}H NMR spectrum of **1**

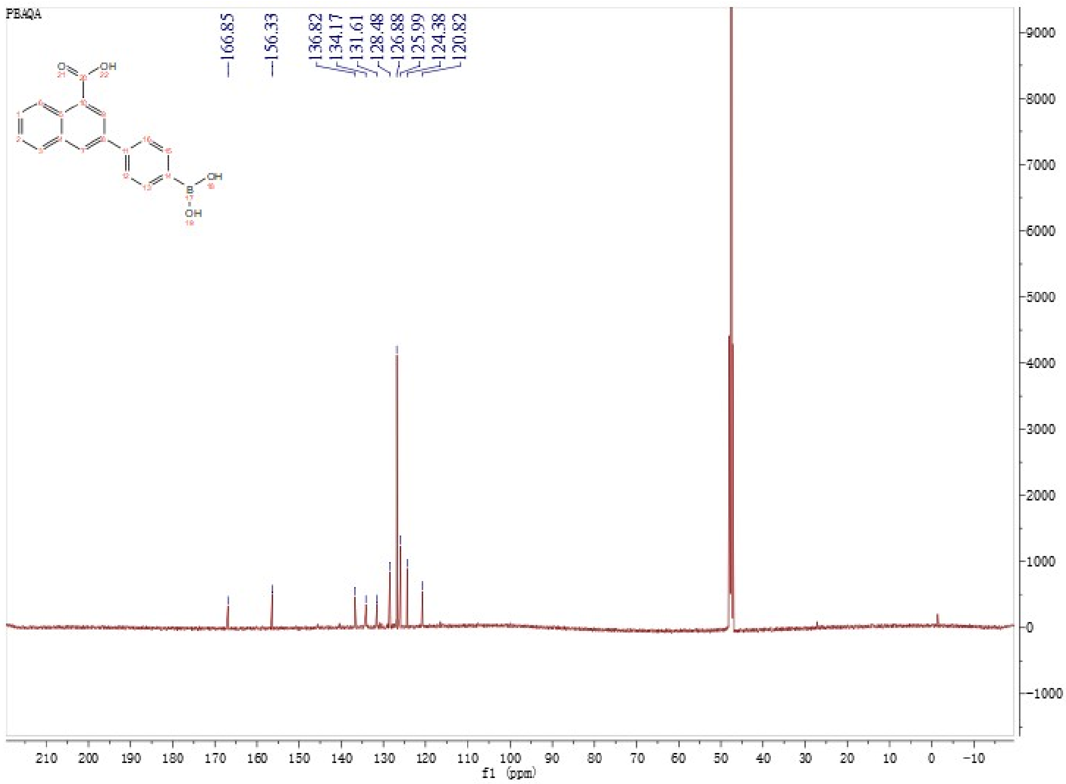

Fig. S2 ^{13}C NMR spectrum of **1**

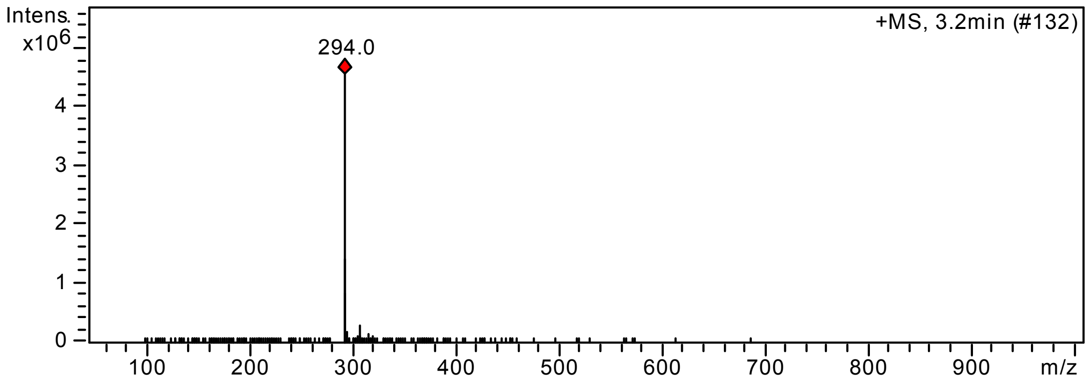

Fig. S3 ESI-MS spectrum of **1**

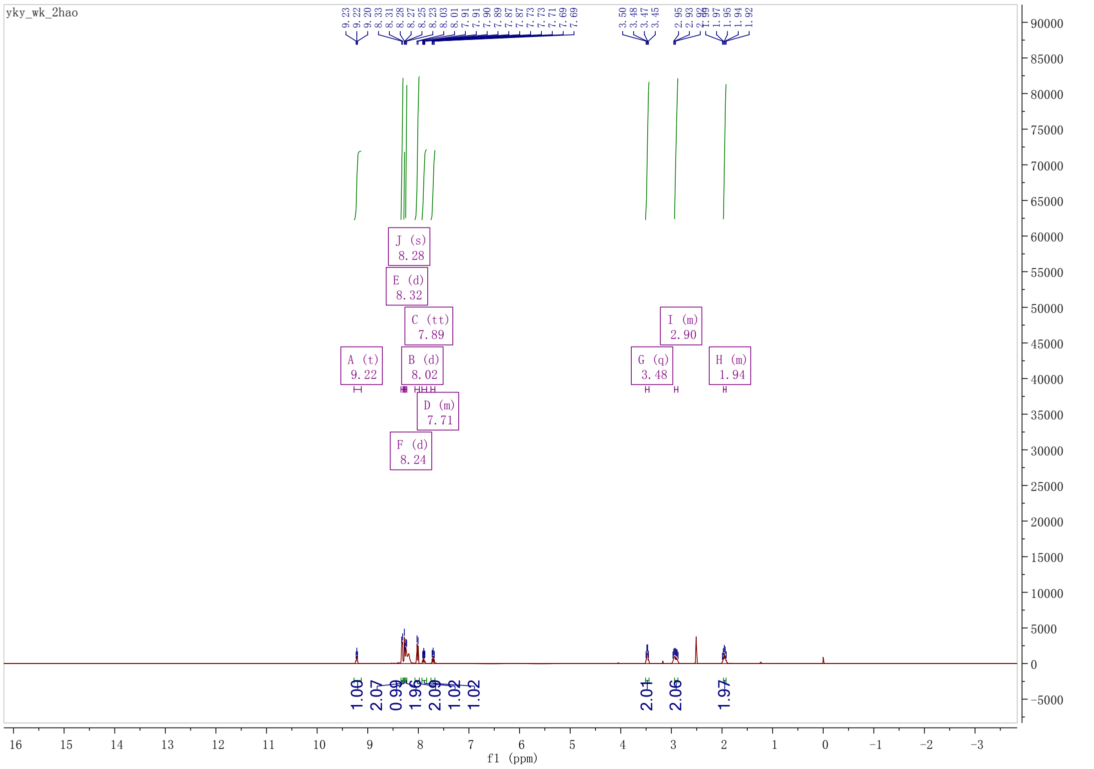

Fig. S4 ^{1}H NMR spectrum of compound **4**

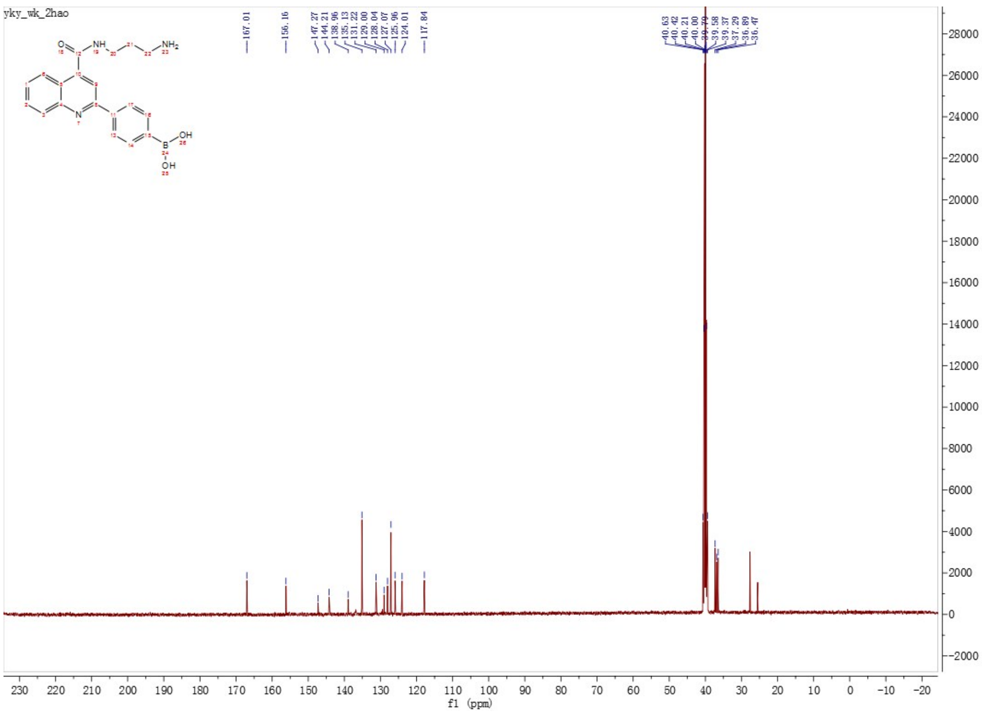

Fig. S5 ^{13}C NMR spectrum of compound **4**

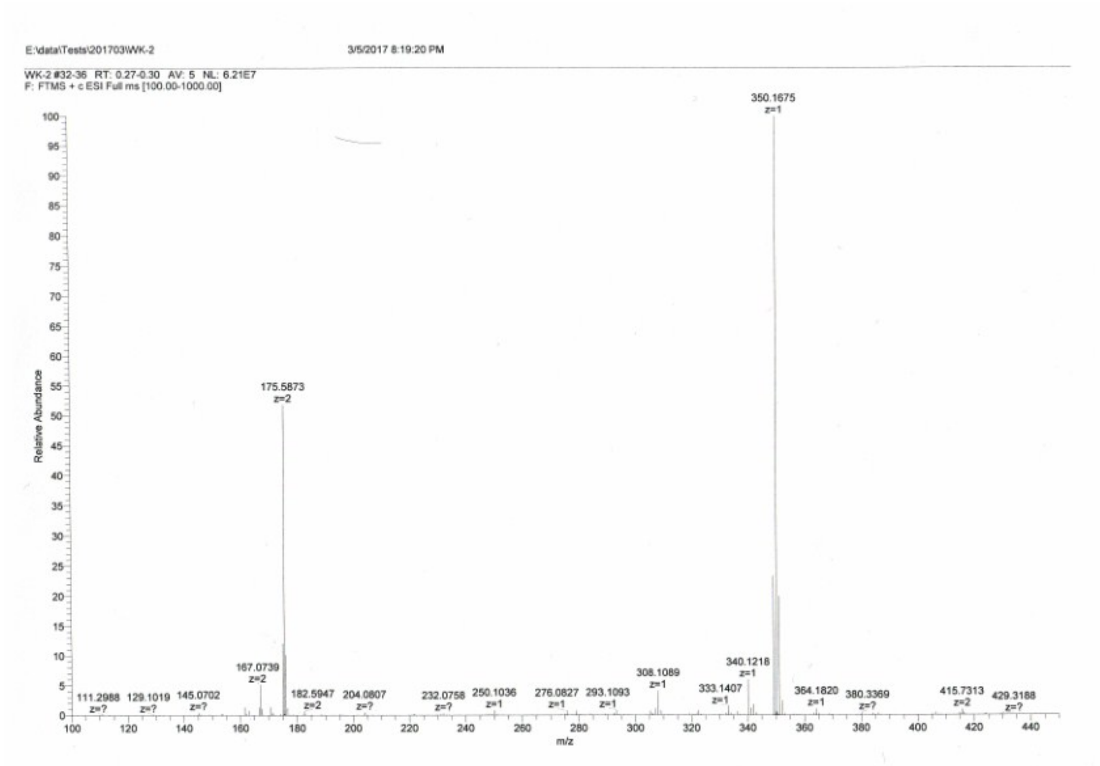

Fig. S6 HRMS spectrum of compound **4**

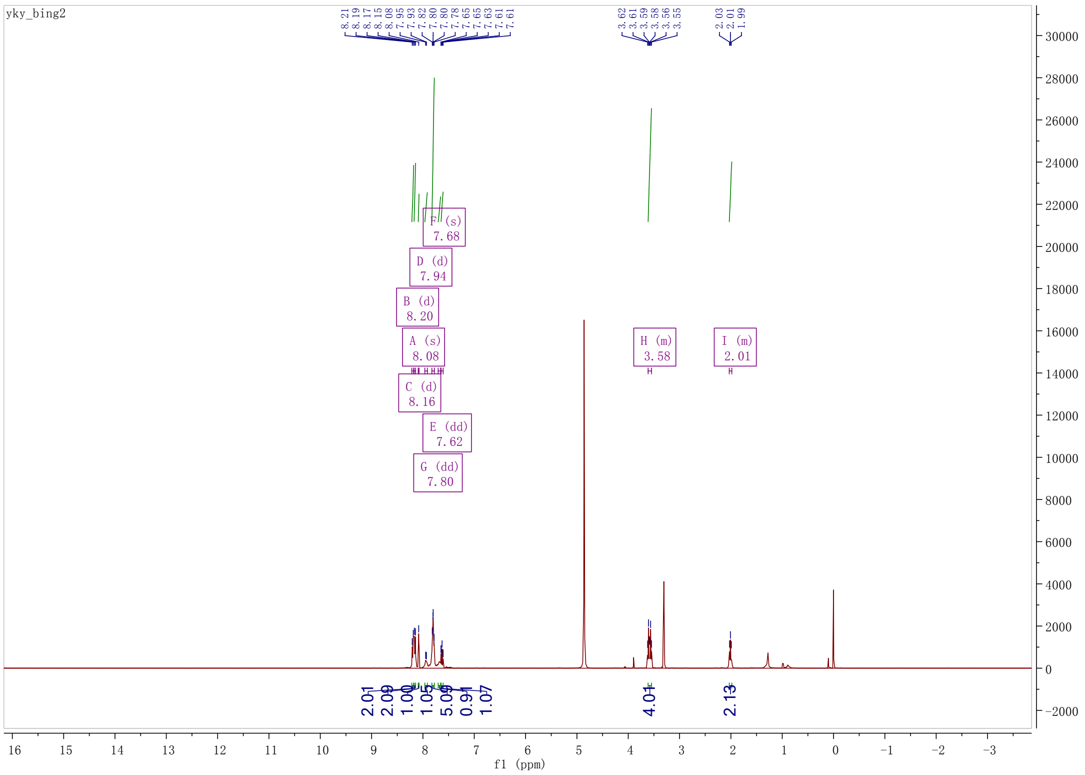

Fig. S7 ^{1}H NMR spectrum of sensor **6**

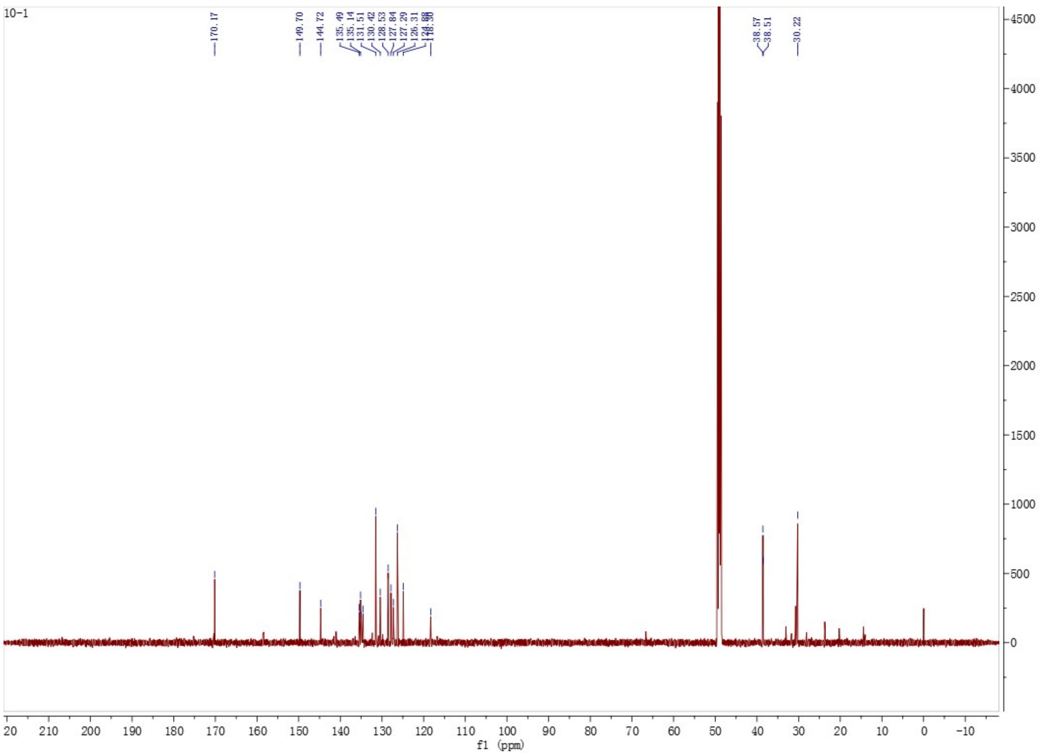

Fig. S8 ^{13}C NMR spectrum of sensor **6**

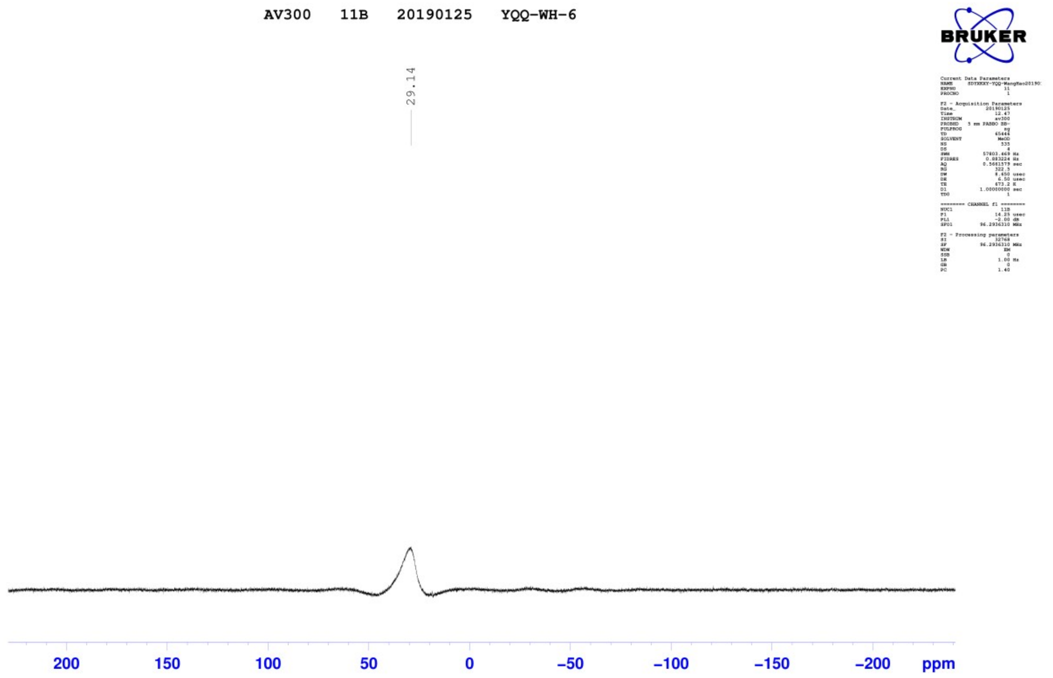

Fig. S9 ^{11}B NMR spectrum of sensor **6**

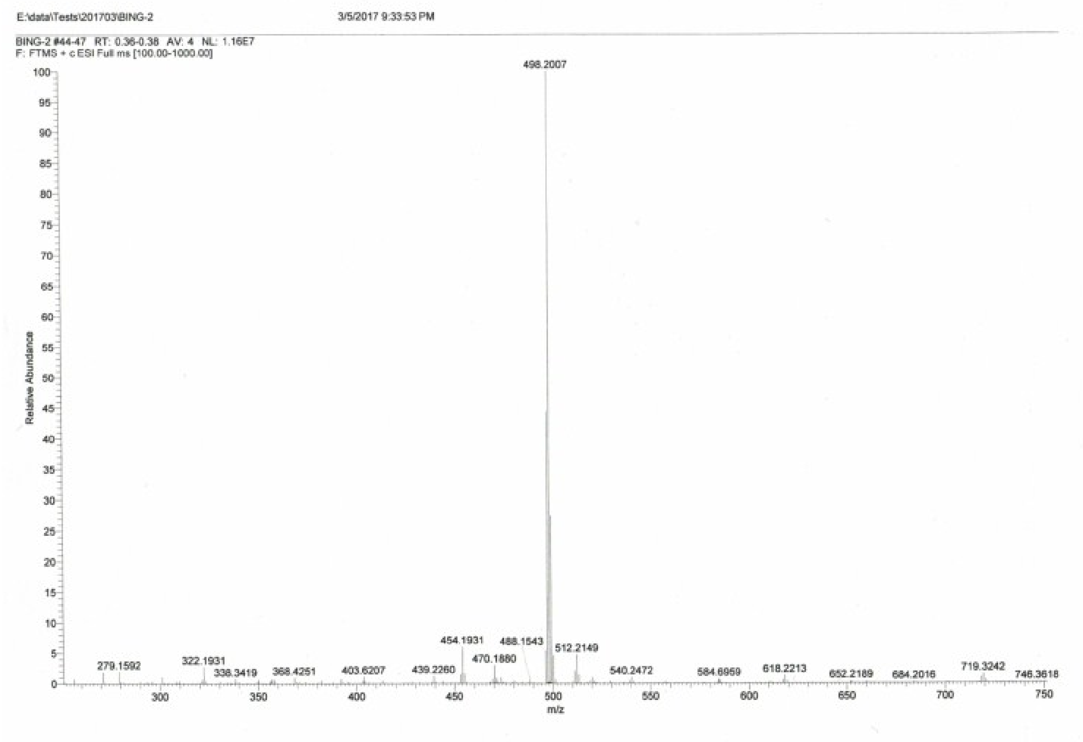

Fig. S10 HRMS spectrum of sensor **6**

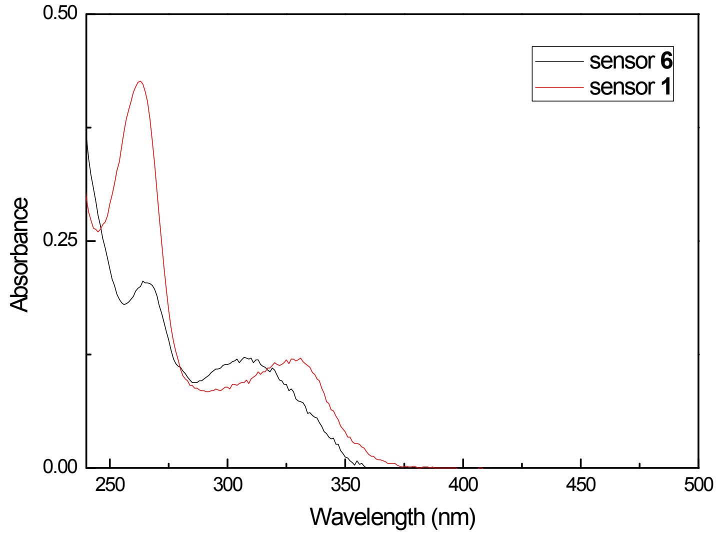

Fig. S11 UV-Vis absorption spectra of sensor **1** and **6** (10^{-5} M) in DMSO/H_2O (1:100, v/v)

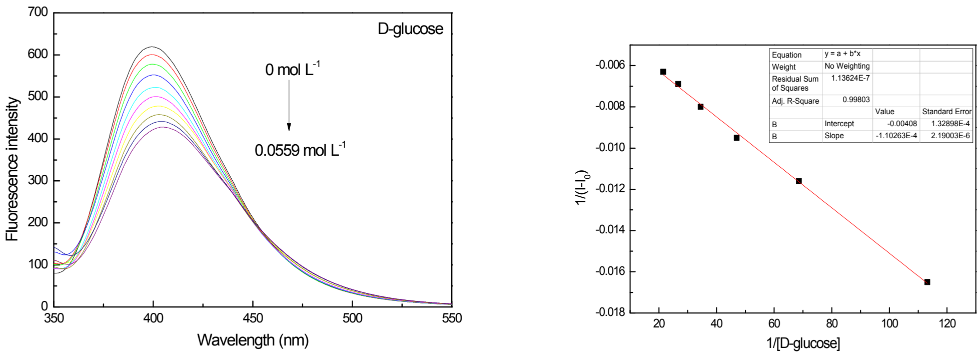

Fig. S12 Fluorescence response of sensor **6** (10^{-5} M) with increasing D-glucose concentration (0 M to 0.0559 M) in DMSO/H_2O (1:100, v/v, pH = 7.4, phosphate buffer, 0.1 M) and Benesi–Hildebrand plot of sensor **6** $1/(I - I_0)$ versus 1/[D-glucose]

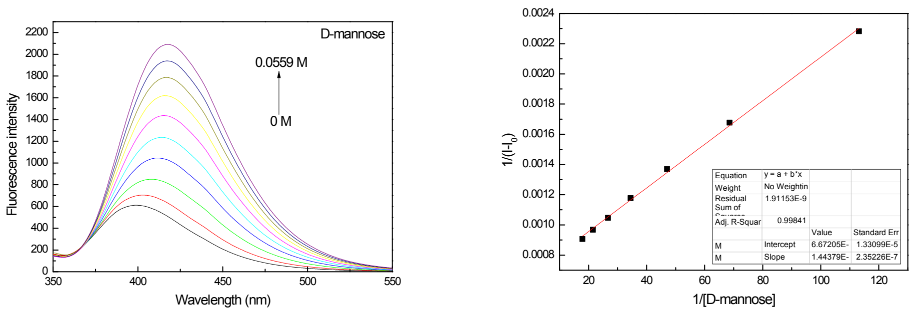

Fig. S13 Fluorescence response of sensor **6** (10^{-5} M) with increasing D-mannose concentration (0 M to 0.0559 M) in DMSO/H_2O (1:100, v/v, pH = 7.4, phosphate buffer, 0.1 M) and Benesi–Hildebrand plot of sensor **6** $1/(I - I_0)$

versus 1/[D-mannose]

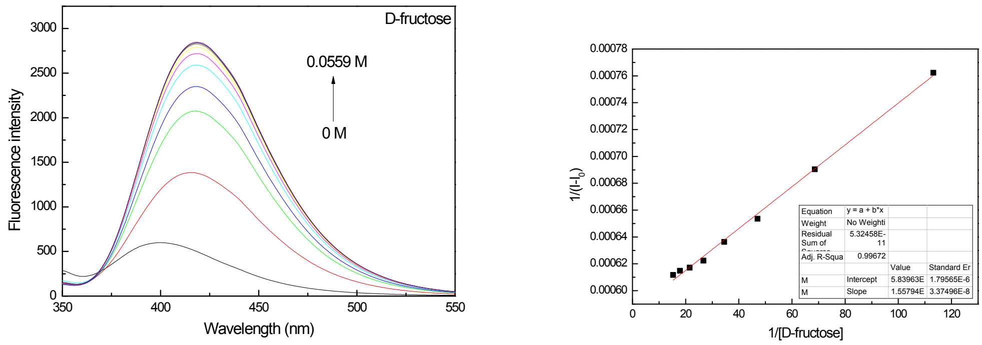

Fig. S14 Fluorescence response of sensor **6** (10^{-5} M) with increasing D-fructose concentration (0 M to 0.0559 M) in DMSO/H_2O (1:100, v/v, pH = 7.4, phosphate buffer, 0.1 M) and Benesi–Hildebrand plot of sensor **6** 1/(I - I_0) versus 1/[D-fructose]

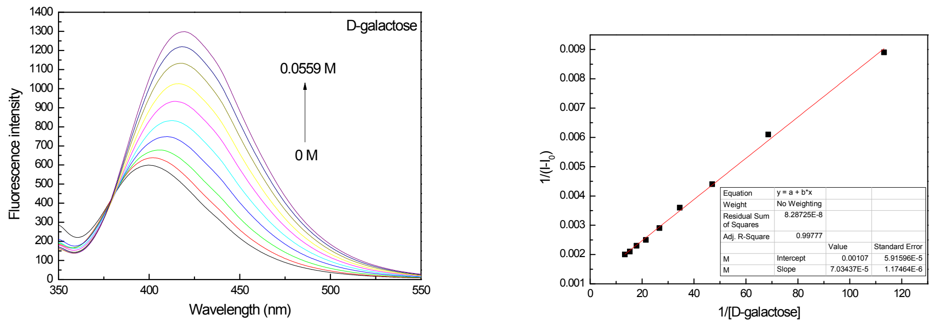

Fig. S15 Fluorescence response of sensor **6** (10^{-5} M) with increasing D-galactose concentration (0 M to 0.0559 M) in DMSO/H_2O (1:100, v/v, pH = 7.4, phosphate buffer, 0.1 M) and Benesi–Hildebrand plot of sensor **6** 1/(I - I_0) versus 1/[D-galactose]

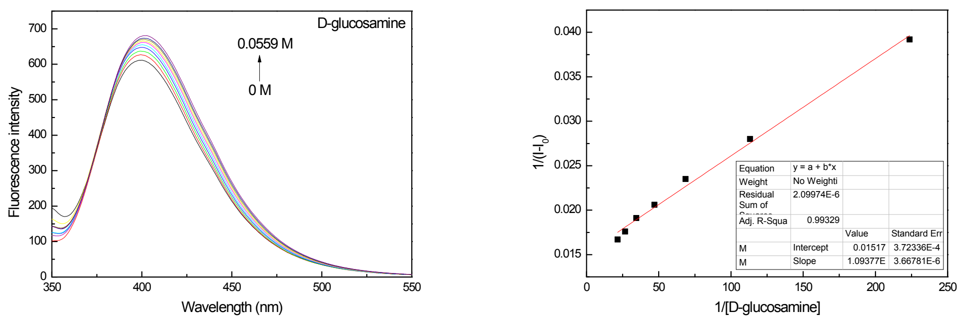

Fig. S16 Fluorescence response of sensor **6** (10^{-5} M) with increasing D-glucosamine concentration (0 M to 0.0559 M) in DMSO/H_2O (1:100, v/v, pH = 7.4, phosphate buffer, 0.1 M) and Benesi–Hildebrand plot of sensor **6** 1/(I - I_0) versus 1/[D-glucosamine]

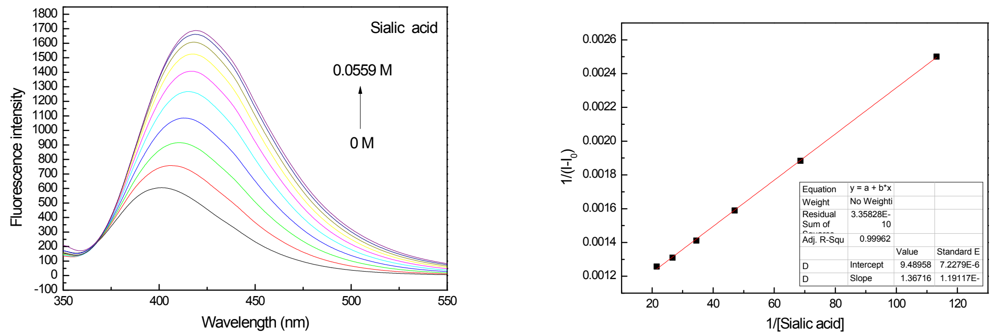

Fig. S17 Fluorescence response of sensor **6** (10^{-5} M) with increasing sialic acid concentration (0 M to 0.0559 M) in DMSO/H_2O (1:100, v/v, pH = 7.4, phosphate buffer, 0.1 M) and Benesi–Hildebrand plot of sensor **6** 1/(I - I_0) versus 1/[Sialic acid]

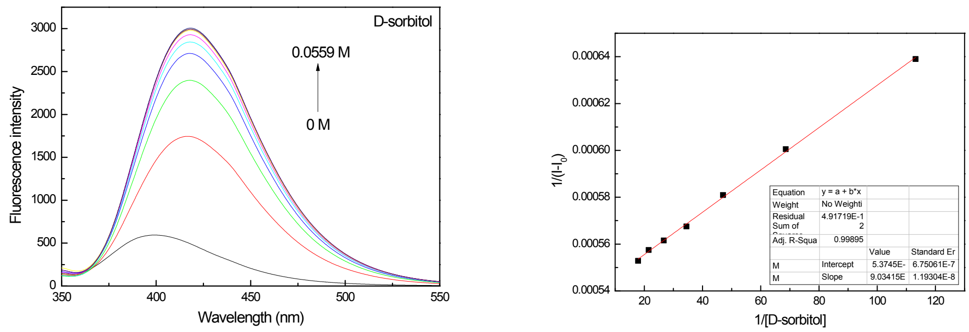

Fig. S18 Fluorescence response of sensor **6** (10^{-5} M) with increasing D-sorbitol concentration (0 M to 0.0559 M) in DMSO/H_2O (1:100, v/v, pH = 7.4, phosphate buffer, 0.1 M) and Benesi–Hildebrand plot of sensor **6** 1/(I - I_0) versus 1/[D-sorbitol]

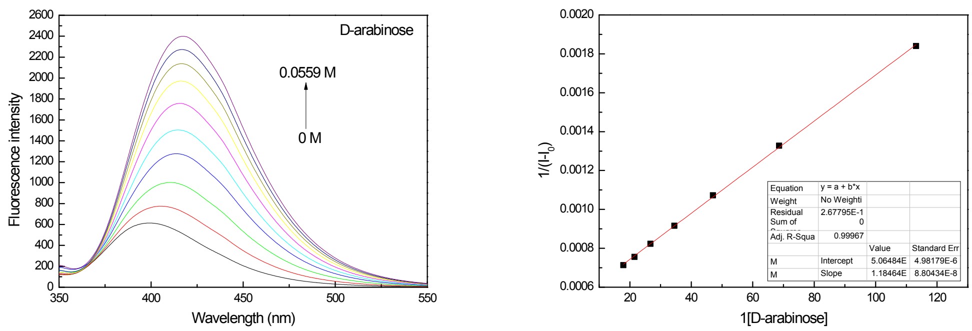

Fig. S19 Fluorescence response of sensor **6** (10^{-5} M) with increasing D-arabinose concentration (0 M to 0.0559 M) in DMSO/H_2O (1:100, v/v, pH = 7.4, phosphate buffer, 0.1 M) and Benesi–Hildebrand plot of sensor **6** 1/(I - I_0) versus 1/[D-arabinose]

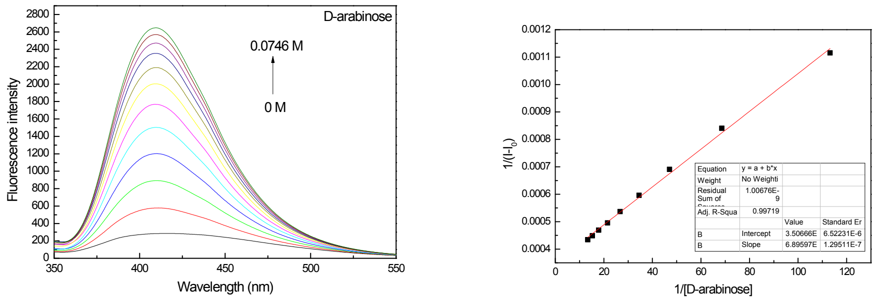

Fig. S20 Fluorescence response of sensor **1** (10^{-5} M) with increasing D-arabinose concentration (0 M to 0.0746 M) in DMSO/H_2O (1:100, v/v, pH = 7.4, phosphate buffer, 0.1 M) and Benesi–Hildebrand plot of sensor **1** $1/(I - I_0)$ versus 1/[D-arabinose]

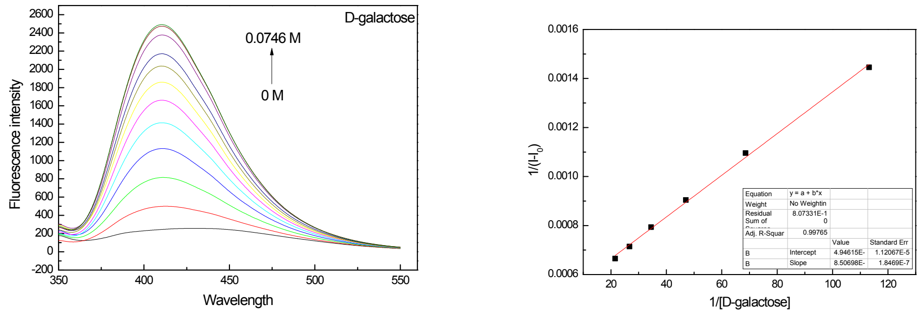

Fig. S21 Fluorescence response of sensor **1** (10^{-5} M) with increasing D-galactose concentration (0 M to 0.0746 M) in DMSO/H_2O (1:100, v/v, pH = 7.4, phosphate buffer, 0.1 M) and Benesi–Hildebrand plot of sensor **1** $1/(I - I_0)$ versus 1/[D-maltose]

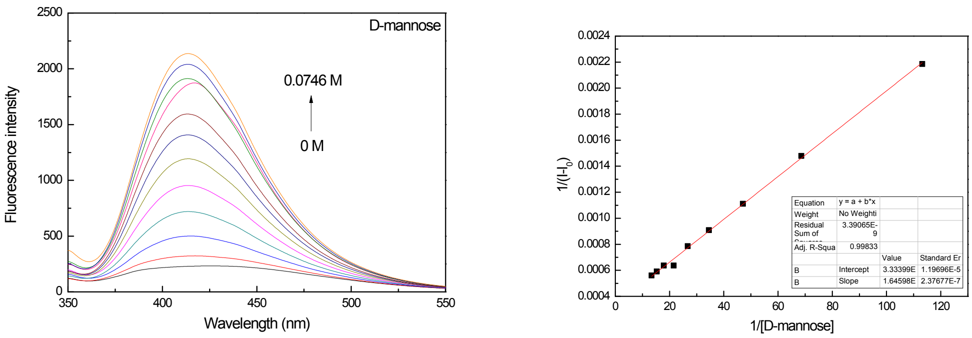

Fig. S22 Fluorescence response of sensor **1** (10^{-5} M) with increasing D-mannose concentration (0 M to 0.0749 M) in DMSO/H_2O (1:100, v/v, pH = 7.4, phosphate buffer, 0.1 M) and Benesi–Hildebrand plot of sensor **1** $1/(I - I_0)$ versus 1/[D-mannose]

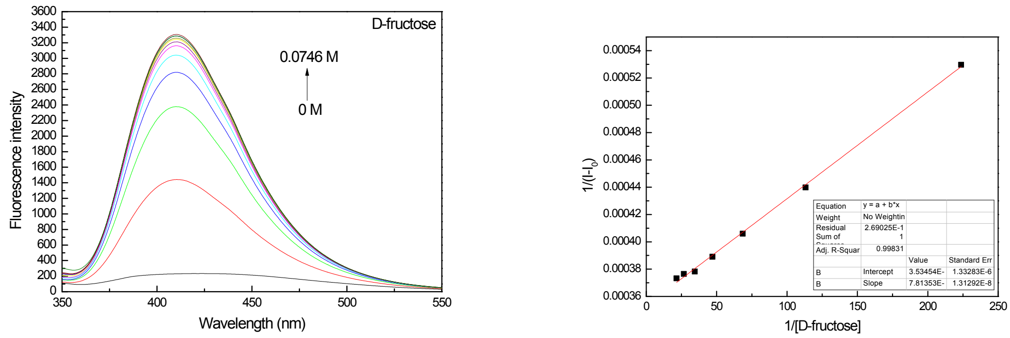

Fig. S23 Fluorescence response of sensor **1** (10^{-5} M) with increasing D-frutose concentration (0 M to 0.0746 M) in DMSO/H_2O (1:100, v/v, pH = 7.4, phosphate buffer, 0.1 M) and Benesi–Hildebrand plot of sensor **1** 1/(I - I_0) versus 1/[D-fructose]

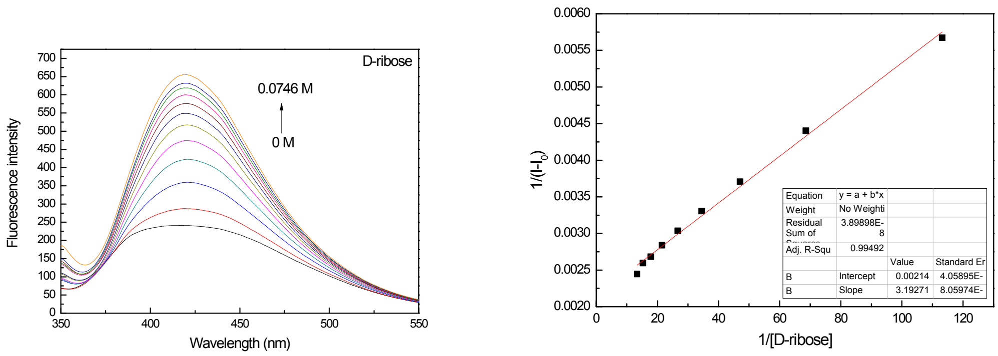

Fig. S24 Fluorescence response of sensor **1** (10^{-5} M) with increasing D-ribose concentration (0 M to 0.0746 M) in DMSO/H_2O (1:100, v/v, pH = 7.4, phosphate buffer, 0.1 M) and Benesi–Hildebrand plot of sensor **1** 1/(I - I_0) versus 1/[D-ribose]

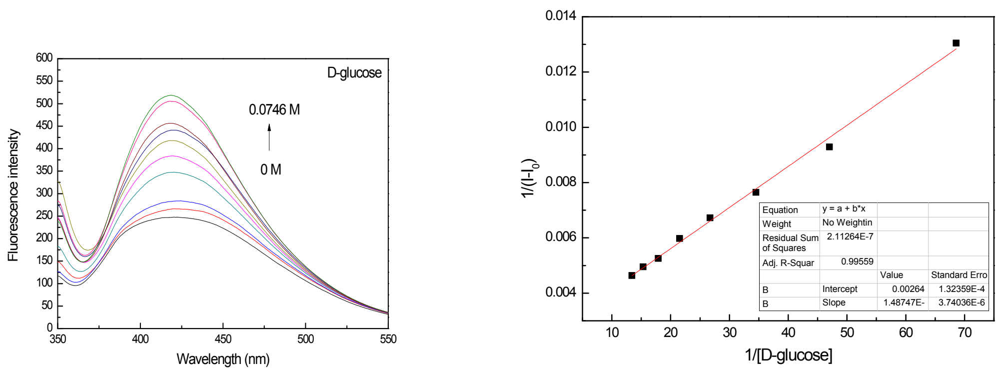

Fig. S25 Fluorescence response of sensor **1** (10^{-5} M) with increasing D-glucose concentration (0 M to 0.0746 M) in DMSO/H_2O (1:100, v/v, pH = 7.4, phosphate buffer, 0.1 M) and Benesi–Hildebrand plot of sensor **1** 1/(I - I_0) versus 1/[D-glucose]

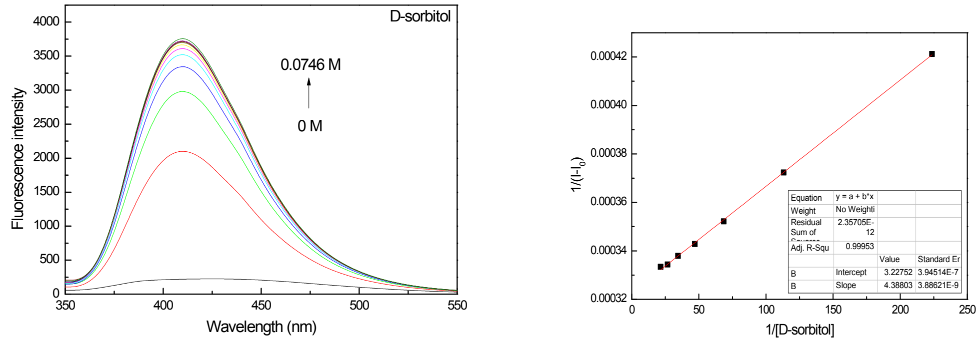

Fig. S26 Fluorescence response of sensor **1** (10^{-5} M) with increasing D-sorbitol concentration (0 M to 0.0746 M) in DMSO/H_2O (1:100, v/v, pH = 7.4, phosphate buffer, 0.1 M) and Benesi–Hildebrand plot of sensor **1** $1/(I - I_0)$ versus 1/[D-sorbitol]

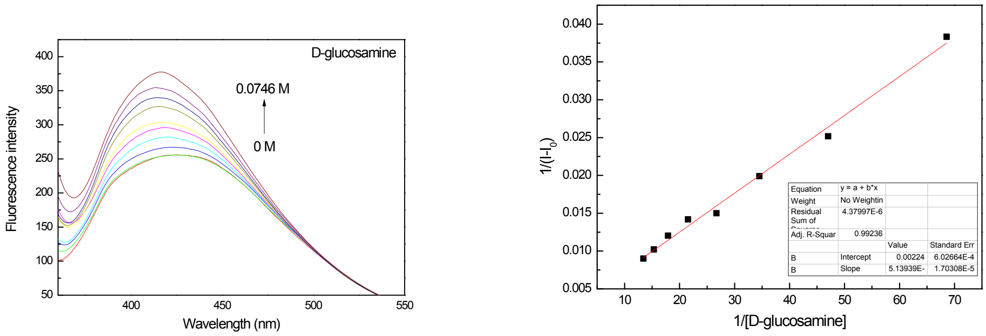

Fig. S27 Fluorescence response of sensor **1** (10^{-5} M) with increasing D-glucosamine concentration (0 M to 0.0746 M) in DMSO/H_2O (1:100, v/v, pH = 7.4, phosphate buffer, 0.1 M) and Benesi–Hildebrand plot of sensor **1** $1/(I - I_0)$ versus 1/[D-glucosamine]

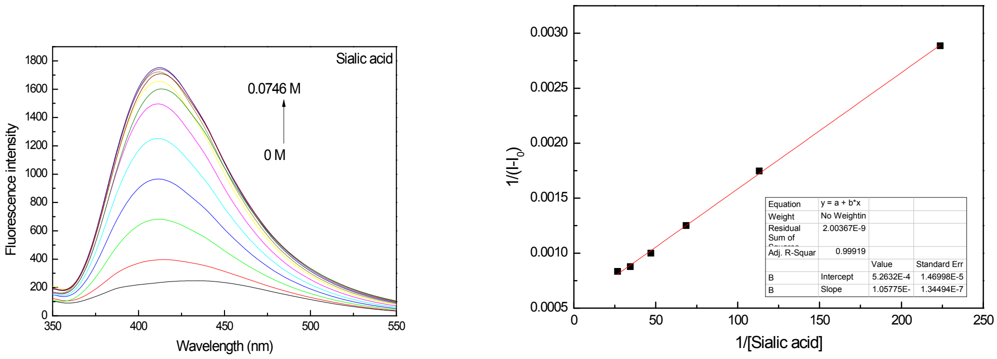

Fig. S28 Fluorescence response of sensor **1** (10^{-5} M) with increasing sialic acid concentration (0 M to 0.0746 M) in DMSO/H_2O (1:100, v/v, pH = 7.4, phosphate buffer, 0.1 M) and Benesi–Hildebrand plot of sensor **1** $1/(I - I_0)$ versus 1/[Sialic acid]

1. H. Wang, G. Fang, K. Wang, Z. Wu and Q. Yao, *Analytical Letters*, 2018, 1-15.